therapy is being explored in the worldwide, prospective, randomized trial GCIG/JGOG 3017, a study designed to compare the survival of patients with ovarian clear cell carcinoma treated either with the paclitaxel-carboplatin combination or the irinotecan-cisplatin combination.

It is well recognized that the dose-limiting toxicities of irinotecan-based therapy are severe neutropenia and diarrhea [6]. The active metabolite of irinotecan, SN-38 (7-ethyl-10-hydroxycamptothecin), is glucuronidated by uridine diphosphate glucuronosyltransferase 1As (UGT-1As) including UGT1A1, and inactivated by forming SN-38 glucuronide (SN-38G) [7, 8]. In these UGT1A enzymes, the UGT1A1 protein has the highest ability to glucuronidate SN-38. Genetic variations in the promoter and coding regions of UGT1A1 have been reported to decrease enzyme activity. A polymorphism of UGT1A1, UGT-1A1*28, is a repeat polymorphism in the TATA box of the promoter, and homozygosity for UGT1A1*28 is associated with Gilbert's syndrome, which is characterized by elevated serum levels of unconjugated bilirubin [9]. Patients bearing the UGT1A1*28 allele have a decreased ability to form SN-38G, and the UGT1A1*28 allele was significantly correlated with irinotecan-induced toxicities [10–14]. In Asians, the allele frequency of UGT1A1*28 is lower, and UGT1A1*6, another polymorphism of UGT1A1, is much higher in Asians compared with Caucasians or African-Americans [15]. Both UGT1A1*6, a G→A transition at codon 71 (G71R), and UGT1A1*27, a C→A transition at codon 229 (P229Q), are polymorphisms of the UGT1A1 gene located on exon 1 [16] and related with reduced SN-38 glucuronidation activity [17, 18]. Recently, a significant association between UGT-1A1*6 and severe adverse effects following irinotecan-based chemotherapy has been reported [19, 20].

On the other hand, a meta-analysis of 10 patient cohorts treated with medium/high-dose irinotecan demonstrated that the risk of grade 3/4 hematologic toxicity was higher in patients with the UGT1A1*28/*28 genotype than in those with the UGT1A1*1/*1 and UGT-1A1*1/*28 genotype [21]. This significant difference was not observed in patients treated with low-dose of irinotecan (100–125 mg/m^2), a commonly used therapeutic range. However, limitations of the study are possibly the heterogeneity of the patients and the treatment schedule, e.g. supplementation of platinum agents.

In the present study, the effect of UGT1A1 genotypes on toxicity profiles was prospectively investigated in gynecologic cancer patients who received the irinotecan-cisplatin combination therapy at the dose and schedule employed in the GCIG/JGOG 3017 trial.

Patients and Methods

Patients and Tumors

Patients meeting the following criteria were eligible for the study: histologically confirmed diagnosis of ovarian or uterine cervical carcinoma; age between 20 and 75 years; a performance status between 0 and 2 on the Eastern Cooperative Oncology Group scale; a life expectancy of at least 3 months; a treatment-free period of at least 4 weeks from the previous chemotherapy or irradiation, and adequate hematological (total white blood cell count ≥3,000/μl; absolute neutrophil count ≥1,500/μl; platelet count ≥100,000/μl and hemoglobin level ≥9 g/dl), hepatic (total bilirubin level ≤1.5 mg/dl, and aspartate and alanine aminotransferase levels ≤3 times the upper limit of normal) and renal (creatinine level ≤1.5 mg/dl and/or creatinine clearance ≥60 ml/min) function. The protocol included the following exclusion criteria: massive ascites and/or massive pleural effusion; serious infectious diseases or other complications such as uncontrollable diabetes, intestinal pneumonitis or bowel obstruction; active bowel bleeding or colitis; active concurrent malignancies; symptomatic brain metastasis; lacting or pregnant women; medical record of hypersensitivity reaction to irinotecan or platinum agents, or other medical problems severe enough to prevent compliance with the present protocol. The study protocol was approved by each institutional review board; the National Defense Medical College, the Saitama Cancer Center, the International Medical Center of the Saitama Medical University and the Nishisaitama Chuo Hospital. All study participants gave informed consent prior to the enrollment in the study.

Drug Administration

The enrolled patients received chemotherapy consisting of 90-min intravenous infusions of irinotecan (60 mg/m^2) on days 1, 8 and 15 and subsequently 120-min intravenous infusions of cisplatin (60 mg/m^2) on day 1 every 4 weeks. Treatment with irinotecan was withheld on days 8 or 15 if the patient experienced hematologic toxicities of grade 3 or more or non-hematologic toxicities of grade 2 or more. A subsequent cycle of chemotherapy was initiated if the patients showed adequate hematological, hepatic and renal function according to the criteria for patient enrollment and did not meet the exclusion criteria. The worst toxicity profiles of the initial two chemotherapy courses and adherence to the study protocol were investigated for the present study.

UGT1A1 Genotyping

Serum samples of the study patients were analyzed for polymorphisms of UGT1A1 using the Invader UGT1A1 Molecular Assay (BML, Kawagoe, Japan), which enabled genotyping of UGT1A1*28, *6, and *27 [22]. Wild-type and non-wild-type UGT1A1 was determined by the assay.

Response Evaluation

Response was evaluated with CT or MR images after two cycles of chemotherapy in the patients with measurable disease. Tumor response was assessed using Response Evaluation Criteria in Solid Tumors [23]. Responses were confirmed by CT at least 4 weeks later. Response evaluation of chemotherapy was not done by serum levels of CA125 in patients with ovarian carcinoma in the present study.

Table 1. Characteristics of the patients

Characteristics	Patients	Median (range)
Total patients	30	
Ovarian cancer	24 (80%)	
Cervical cancer	6 (20%)	
Age, years		58 (37–75)
Weight, kg		51 (42–75)
Performance status (ECOG)		
0	25 (83%)	
1	5 (17%)	
2	0 (0%)	
Previous chemotherapy		
≥2 regimens	14 (47%)	
1 regimen	13 (43%)	
No	3 (10%)	
Previous pelvic radiotherapy		
Yes	3 (10%)	
No	27 (90%)	

ECOG = Eastern Cooperative Oncology Group.

Table 2. UGT1A1 genotype and total bilirubin level prior to therapy and the highest value during chemotherapy

UGT1A1 genotype	Bilirubin prior mean (range)	Bilirubin highest mean (range)	p value[1]
Wild type (n = 17)	0.49 (0.2–0.7)	0.78 (0.3–2.1)	<0.01
Non-wild type (n = 13)	0.61 (0.3–1.2)	0.79 (0.3–1.2)	0.14
UGT1A1*28 (n = 4)	0.60 (0.4–1.0)	0.80 (0.4–1.2)	0.52
UGT1A1*6 (n = 8)	0.56 (0.3–1.2)	0.78 (0.3–1.2)	0.83
UGT1A1*6*28 (n = 1)	1.0	0.9	–
p value[2]	0.02	0.72	

[1] Comparing the bilirubin levels noted prior to chemotherapy with the highest value obtained during chemotherapy.

[2] Comparing serum bilirubin levels of cases with UGT1A1 wild-type with those with the non-wild-type genotype (UGT1A1*28, *6 and *6*28).

Toxicity Profiles and Statistical Analysis

Physical examination and serum blood tests were carried out on days 1, 3, 8, 15 and 21 for toxicity evaluation. Toxicity was assessed using the National Cancer Institute Common Toxicity Criteria (version 3). The χ^2 test and Student's t test for unpaired data were used for statistical analyses. Multivariate logistic regression analyses of toxicities were performed using StatView (version 5.0; SAS Institute, Cary, N.C., USA). A p value <0.05 was considered statistically significant.

Results

A total of 30 patients who fulfilled the inclusion criteria but not the exclusion criteria were investigated. Table 1 summarizes the characteristics of the patients enrolled in the study. No case was excluded due to insufficient liver and renal function. All the 30 patients were Japanese. UGT1A1 genotyping using the Invader UGT1A1 Molecular Assay revealed the wild type in 17 patients (57%), UGT1A1*28 in 4 (13%), UGT1A1*6 in 8 (27%) and UGT1A1*28*6 in 1 (3%) patient; UGT1A1*27 was not detected in any of the 30 study patients. All UGT1A1 polymorphisms were heterozygous alterations, and no homozygous polymorphisms were observed in the present study.

Possible correlations between the total serum bilirubin level prior to and the highest serum bilirubin level during the chemotherapy and UGT1A1 genotypes were assessed. The results are summarized in table 2. Serum levels of bilirubin were higher in patients with UGT1A1 non-wild type genotypes in comparison with those with the wild type (p = 0.02). Serum bilirubin levels were significantly increased after chemotherapy in the UGT1A1 wild-type cases. In UGT1A1 non-wild-type patients, serum bilirubin levels were slightly increased after chemotherapy, but the differences were not significant.

Response was assessable in 13 of 17 UGT1A1 wild-type patients, and 10 of 13 patients with UGT1A1 non-wild-type genotype. The patients with UGT1A1 wild type included 3 (23%) patients with partial responses, 6 (54%) with stable disease and 3 (23%) with progressive disease. The UGT1A1 non-wild-type group comprised 3 (30%) patients with partial responses, 4 (40%) with stable disease and 3 (30%) with progressive disease. A complete response was not observed in the present study cohort. Overall response amounted to 23% in the wild-type group and to 30% in the non-wild-type group, with no significant difference between both groups (p = 0.71).

The overall toxicity profiles according to UGT1A1 genotypes are shown in table 3. There was a marked increase in grade 3/4 toxicities in the UGT1A1 non-wild-type group. Neutropenia (p = 0.04), thrombocytopenia (p = 0.04) and diarrhea (p = 0.005) were more frequently observed in the UGT1A1 non-wild-type group. Other non-hematologic grade 3/4 toxicities including renal function were not observed. Toxicity-induced discon-

Table 3. Associations between UGT1A1 genotypes and grade 3–4 toxicities or discontinuation (days 8 and 15)/delay of chemotherapy

UGT1A1 genotype	Leukopenia	Neutropenia	Thrombocytopenia	Nausea	Vomiting	Diarrhea	Discontinuation of irinotecan	Delay of the second cycle
Wild type (n = 17)	1 (6%)	4 (24%)	0 (0%)	2 (12%)	5 (29%)	0 (0%)	5 (29%)	2 (12%)
Non-wild type (n = 13)	4 (31%)	8 (62%)	3 (23%)	5 (38%)	6 (46%)	5 (38%)	10 (77%)	4 (31%)
UGT1A1*28 (n = 4)	1 (25%)	1 (25%)	1 (25%)	2 (50%)	3 (75%)	1 (25%)	3 (75%)	1 (25%)
UGT1A1*6 (n = 8)	2 (25%)	6 (75%)*	2 (25%)*	3 (38%)	3 (38%)	4 (50%)*	6 (75%)*	3 (38%)
UGT1A1*28*6 (n = 1)	1 (100%)	1 (100%)	0 (0%)	0 (0%)	0 (0%)	0 (0%)	1 (100%)	0 (0%)
p value[1]	0.07	0.04	0.04	0.09	0.35	0.005	0.01	0.19

* $p < 0.05$, UGT1A1*6 vs. wild type.
[1] Comparing the frequencies of events in cases with UGT1A1 wild-type and those with UGT1A1 non-wild-type genotypes.

Table 4. Multiple logistic regression analysis of the occurrence of grade 3/4 neutropenia in all cases and cases with UGT1A1*6 and wild-type genotype[1]

Variables	Hazard ratio	95% confidence interval	p value
All cases			
Age			0.23
≤55 years	1		
≥56 years	0.66	0.11; 4.11	
Previous chemotherapy			0.50
≤1 regimen	1		
≥2 regimen	3.43	0.40; 29.33	
Previous pelvic radiotherapy			0.017
No	1		
Yes	7.80	1.72; 35.37	
UGT1A1 genotype			0.007
Wild type (n = 17)	1		
Non-wild type (n = 8)	7.85	2.05; 57.40	
*Cases with UGT1A1*6 and wild-type genotype*			
Age			0.67
≤55 years	1		
≥56 years	0.55	0.04; 7.24	
Previous chemotherapy			0.48
≤1 regimen	1		
≥2 regimen	2.08	0.21; 27.02	
Previous pelvic radiotherapy			0.13
No	1		
Yes	3.04	0.89; 24.44	
UGT1A1 genotype			0.03
Wild type (n = 17)	1		
UGT1A1*6 (n = 8)	10.06	1.14; 88.98	

[1] Worst toxicities in the initial two courses.

Table 5. Multiple logistic regression analysis of the occurrence of grade 3/4 diarrhea in all cases and cases with UGT1A1*6 and wild-type genotype[1]

Variables	Hazard ratio	95% confidence interval	p value
All cases			
Age			0.15
≤55 years	1		
≥56 years	1.05	0.20; 5.12	
Previous chemotherapy			0.46
≤1 regimen	1		
≥2 regimen	3.42	0.41; 27.40	
Previous pelvic radiotherapy			0.03
No	1		
Yes	6.00	1.58; 22.77	
UGT1A1 genotype			0.002
Wild type (n = 17)	1		
Non-wild type (n = 13)	6.54	1.44; 29.60	
*Cases with UGT1A1*6 and wild-type genotype*			
Age, years			0.19
≤55 years	1		
≥56 years	1.21	0.18; 5.56	
Previous chemotherapy			0.71
≤1 regimen	1		
≥2 regimen	2.00	0.05; 38.46	
Previous pelvic radiotherapy			0.14
No	1		
Yes	3.65	0.78; 30.11	
UGT1A1 genotype			0.001
Wild type (n = 17)	1		
UGT1A1*6 (n = 8)	7.45	1.44; 29.78	

[1] Worst toxicities in the initial two courses.

tinuation of irinotecan administration on days 8 and/or 15 was significantly higher in the non-wild type group ($p = 0.01$). Compared with the wild-type patients, UGT1A1*6 patients showed a significantly higher rate of grade 3/4 neutropenia ($p = 0.014$), thrombocytopenia ($p = 0.03$) and diarrhea ($p < 0.001$), and irinotecan treatment was more often modified ($p = 0.03$). There was no statistically significant relationship between response and the frequency of grade 3/4 toxicity (data not shown).

Multiple logistic regression analysis of the occurrence of grade 3/4 neutropenia (table 4) or grade 3/4 diarrhea (table 5) revealed a significant, independent association with the UGT1A1 non-wild type. In addition to the UGT1A1 genotype, previous pelvic radiotherapy was also identified as an independent factor for neutropenia and diarrhea in the analysis of all cases (upper part of table 4, 5). There was no significant relationship with the UGT1A1 genotype and other toxicities including thrombocytopenia by multivariate analysis (data not shown).

Further, excluding 4 patients with UGT1A1*28 and 1 with UGT1A1*28*6, using multiple logistic regression, the incidence of grade 3/4 toxicities was analyzed using age, previous chemotherapy, previous pelvic radiotherapy and UGT1A1 genotype (UGT1A1*6 vs. wild type) as variables. The UGT1A1*6 genotype was identified as an independent risk factor for grade 3/4 neutropenia (hazard ratio, 6.54; 95% confidence interval, 1.44–29.60) and grade 3/4 diarrhea (hazard ratio, 7.45; 95% confidence interval, 1.44–29.78; lower part in table 4, 5). Age, previous chemotherapy and previous pelvic radiotherapy were not significant risk factors in these analyses.

Discussion

There have been reports of more than hundred polymorphisms in the UGT1A1 gene [24]. UGT1A1*6, a UGT polymorphism, is one of the single nucleotide polymorphisms on the exon 1 coding region of the UGT1A1 gene. There is marked ethnical difference in the allele frequencies of UGT1A1*28 and UGT1A1*6 [15, 19]. The allele frequency of UGT1A1*28 is 30–40% in Caucasians and approximately 10% in Asians. Conversely, the UGT1A1*6 allele is observed in ~20% of Asians, but it is rarely detected in Caucasians. It is suggested that UGT1A1*6 is not negligible in clinical studies using irinotecan-based regimens in Asian patients. In the present study, UGT1A1*6 was noted in 8 cases (27%) and UGT1A1*28 in 4 cases (13%), supporting the higher incidence of the UGT1A1*6 polymorphism in Asians.

A previous report described the significant increase in the basal level of serum total bilirubin in UGT1A1*28 or UGT1A1*6 patients [20]. In our cases, serum total bilirubin was significantly higher in non-wild-type patients compared with wild-type cases, but the levels did not exceed the upper limit of normal. The present data support the potential capability of distinguishing patients with the UGT1A1 non-wild type genotype by their serum total bilirubin level. The serum total bilirubin level was elevated in both patient groups during chemotherapy, being in line with previous observations [10]. However, only in wild-type patients the difference was significant. The lack of significance in non-wild type patients might be due to the small number of cases.

In the present study, response rates to the irinotecan-cisplatin combination were similar in both UGT1A1 wild-type and non-wild-type patients. A significant correlation between homozygous UGT1A1*6 and lower tumor response to irinotecan-based chemotherapy has already been reported in Korean patients [19]. Although a significant correlation between UGT1A1 polymorphisms and tumor response was not observed in the present study, further investigations in a larger patient cohort are needed to evaluate the association between the UGT1A1 genotype and tumor response.

In the present study, previous pelvic radiotherapy was found to be a significant predictor of grade 3/4 neutropenia or diarrhea in multivariate analysis: 3 cases of cervical cancer had been treated with whole pelvic irradiation at a total dose of 50 Gy. Two of the 3 cases included patients with UGT1A1 non-wild type genotypes; a case with UGT1A1*6 and another with UGT1A1*28. Additionally, all 3 cases had received previous chemotherapy consisting of more than two regimens. Grade 3/4 neutropenia was observed in all 3 cases, and grade 3/4 diarrhea occurred in 2 cases with UGT1A1 non-wild-type genotypes. Possibly, previous heavy treatment with radiotherapy and chemotherapy affected the results in these 3 cases. However, multivariate analysis demonstrated that previous pelvic radiotherapy was significantly associated with severe toxicities.

The second significant predictor of severe toxicities in the present study was the UGT1A1 non-wild-type genotype. The relationship between the UGT1A1*28 genotype and toxicity resulting from irinotecan-based chemotherapy has already been established. On the other hand, a previous large retrospective investigation had failed to find a significant association between UGT1A1*6

and irinotecan-induced toxicity [9], but recent studies have described a positive relationship of the UGT1A1*6 genotype and toxicities. Han et al. [19] first reported that the UGT1A1*6 genotype was related with lower SN-38 glucuronidation and a higher frequency of grade 3–4 toxicities in Korean patients who were treated with the irinotecan-cisplatin combination. Sai et al. [20] also documented that the incidence of grade 3/4 neutropenia was significantly higher in patients with the UGT1A1*6 genotype who were treated with irinotecan-based chemotherapy. In line with these observations, the present study revealed a significant association of UGT1A1*6 not only with hematological toxicity but also with life-threatening diarrhea. The results of our case series were in contrast to a previous large meta-analysis that found no significant contribution of UGT1A1 genotypes to the toxicity profiles in cases treated with low-dose (100–125 mg/m^2) irinotecan monotherapy [21]. The effects of platinum-containing drugs, irinotecan and/or SN-38 on P-glycoprotein expression and function and on human intestinal and biliary transport may enhance toxicity, exceeding possible effects of UGT1A1 polymorphisms and metabolic drug pathways. In a recent study, irinotecan induced P-glycoprotein expression and function in human intestinal epithelial cells [25]. Inversely, administration of cisplatin, which increases P-glycoprotein expression, could modulate the secretory transport of irinotecan and SN-38 [26].

To confirm these observations, studies including pharmacogenomics are needed. A recent study revealed other UGT1A1 polymorphisms, UGT1A1*7 and UGT1A1*9, associated with tumor response [27] and decreased glucuronosyltransferase activity for SN-38 [28]. Additionally, UGT1A1 genotypes affecting the pharmacokinetics of irinotecan-based chemotherapy may also exist. However, the present study demonstrated a significant association of UGT1A1*6 with grade 3/4 neutropenia and grade 3/4 diarrhea in patients treated with cisplatin and low-dose irinotecan. In the clinical setting, genotyping of UGT1A1*6 in addition to UGT1A1*28 is recommendable for patients treated with irinotecan and cisplatin, especially in Asian patients.

References

1 Sugiyama T, Yakushiji M, Nishida T, et al: Irinotecan (CPT-11) combined with cisplatin in patients with refractory or recurrent ovarian cancer. Cancer Lett 1998;128:211–218.
2 Sugiyama T, Yakushiji M, Noda K, et al: Phase II study of irinotecan and cisplatin as first-line chemotherapy in advanced or recurrent cervical cancer. Oncology 2000;58:31–37.
3 Adachi S, Ogasawara T, Yamasaki N, et al: A pilot study of CPT-11 and cisplatin for ovarian clear cell adenocarcinoma. Jpn J Clin Oncol 1999;29:434–437.
4 Kita T, Kikuchi Y, Kudoh K, et al: Exploratory study of effective chemotherapy to clear cell carcinoma of the ovary. Oncol Rep 2000;7:327–331.
5 Takano M, Kikuchi Y, Yaegashi N, et al: Adjuvant chemotherapy with irinotecan hydrochloride and cisplatin for clear cell carcinoma of the ovary. Oncol Rep 2006;16:1301–1306.
6 de Forni M, Bugat R, Chabot GG, et al: Phase I and pharmacokinetic study of the camptothecin derivative irinotecan, administered on a weekly schedule in cancer patients. Cancer Res 1994;54:4347–4354.
7 Iyer L, King CD, Whitington PF, et al: Genetic predisposition to the metabolism of irinotecan (CPT-11). Role of uridine diphosphate glucuronosyltransferase isoform 1A1 in the glucuronidation of its active metabolite (SN-38) in human liver microsomes. J Clin Invest 1998;101:847–854.
8 Ciotti M, Basu N, Brangi M, Owens IS: Glucuronidation of 7-ethyl-10-hydroxycamptothecin (SN-38) by the human UDP-glucuronosyltransferases encoded at the UGT1 locus. Biochem Biophys Res Commun 1999;260:199–202.
9 Bosma PJ, Chowdhury JR, Bakker C, et al: The genetic basis of the reduced expression of bilirubin UDP-glucuronosyltransferase 1 in Gilbert's syndrome. N Engl J Med 1995;333:1171–1175.
10 Ando Y, Saka H, Ando M, et al: Polymorphisms of UDP-glucuronosyltransferase gene and irinotecan toxicity: a pharmacogenetic analysis. Cancer Res 2000;60:6921–6926.
11 Iyer L, Das S, Janisch L, et al: UGT1A1*28 polymorphism as a determinant of irinotecan disposition and toxicity. Pharmacogenomics J 2002;2:43–47.
12 Innocenti F, Undevia SD, Iyer L, et al: Genetic variants in the UDP-glucuronosyltransferase 1A1 gene predict the risk of severe neutropenia of irinotecan. J Clin Oncol 2004;22:1382–1388.
13 Marcuello E, Altés A, Menoyo A, et al: UGT1A1 gene variations and irinotecan treatment in patients with metastatic colorectal cancer. Br J Cancer 2004;91:678–682.
14 Rouits E, Boisdron-Celle M, Dumont A, et al: Relevance of different UGT1A1 polymorphisms in irinotecan-induced toxicity: a molecular and clinical study of 75 patients. Clin Cancer Res 2004;10:5151–5159.
15 Liu JY, Qu K, Sferruzza AD, Bender RA: Distribution of the UGT1A1*28 polymorphism in Caucasian and Asian populations in the US: a genomic analysis of 138 healthy individuals. Anticancer Drugs 2007;18:693–696.
16 Mackenzie PI, Bock KW, Burchell B, et al: Nomenclature update for the mammalian UDP glycosyltransferase (UGT) gene superfamily. Pharmacogenet Genomics 2005;15:677–685.
17 Gagné J-F, Montminy V, Belanger P, et al: Common human UGT1A polymorphisms and the altered metabolism of irinotecan active metabolite 7-ethyl-10-hydroxycamptothecin (SN-38). Mol Pharmacol 2002;62:608–617.
18 Jinno H, Tanaka-Kagawa T, Hanioka N, et al: Glucuronidation of 7-ethyl-10-hydroxycamptothecin (SN-38), an active metabolite of irinotecan (CPT-11), by human UGT1A1 variants, G71R, P229Q, and Y486D. Drug Metab Dispos 2003;31:108–113.

19 Han JY, Lim HS, Shin ES, et al: Comprehensive analysis of UGT1A polymorphisms predictive for pharmacokinetics and treatment outcome in patients with non-small-cell lung cancer treated with irinotecan and cisplatin. J Clin Oncol 2006;24:2237–2244.
20 Sai K, Saito Y, Sakamoto H, et al: Importance of UDP-glucuronosyltransferase 1A1*6 for irinotecan toxicities in Japanese cancer patients. Cancer Lett 2008;261:165–171.
21 Hoskins JM, Goldberg RM, Qu P, et al: UGT-1A1*28 genotype and irinotecan-induced neutropenia: dose matters. J Natl Cancer Inst 2007;99:1290–1295.
22 Hasegawa Y, Sarashina T, Ando M, et al: Rapid detection of UGT1A1 gene polymorphisms by newly developed Invader assay. Clin Chem 2004;50:1479–1480.
23 Therasse P, Arbuck SG, Eisenhauer EA, et al: New guidelines to evaluate the response to treatment in solid tumors (RECIST) guidelines. J Natl Cancer Inst 2000;92:205–216.
24 UGT: UDP-Glucuronosyltransferase Alleles Nomenclature page. Adelaide, Flinders University School of Medicine, accessed May 20, 2008. http://som.flinders.edu.au/FUSA/ClinPharm/UGT/
25 Haslam IS, Jones K, Coleman T, et al: Induction of P-glycoprotein expression and function in human intestinal epithelial cells (T84). Biochem Pharmacol 2008;76:850–861.
26 Bansal T, Awasthi A, Jaggi M, et al: Pre-clinical evidence for altered absorption and biliary excretion of irinotecan (CPT-11) in combination with quercetin: possible contribution of P-glycoprotein. Life Sci 2008;83:250–259.
27 Carlini LE, Meropol NJ, Bever J, et al: UGT-1A7 and UGT1A9 polymorphisms predict response and toxicity in colorectal cancer patients treated with capecitabine/irinotecan. Clin Cancer Res 2005;11:1226–1236.
28 Fujita K, Ando Y, Nagashima F, et al: Genetic linkage of UGT1A7 and UGT1A9 polymorphisms to UGT1A1*6 is associated with reduced activity for SN-38 in Japanese patients with cancer. Cancer Chemother Pharmacol 2007;60:515–522.

Cancer Immunol Immunother (2009) 58:641–652
DOI 10.1007/s00262-008-0585-3

ORIGINAL ARTICLE

Clinical significance of the NKG2D ligands, MICA/B and ULBP2 in ovarian cancer: high expression of ULBP2 is an indicator of poor prognosis

Kui Li · Masaki Mandai · Junzo Hamanishi · Noriomi Matsumura · Ayako Suzuki · Haruhiko Yagi · Ken Yamaguchi · Tsukasa Baba · Shingo Fujii · Ikuo Konishi

Received: 15 May 2008 / Accepted: 25 August 2008 / Published online: 13 September 2008

Abstract
Objective To investigate the clinical significance of the expression of the NKG2D ligands MICA/B and ULBP2 in ovarian cancer.
Methods Eighty-two ovarian cancer patients and six patients without ovarian cancer from Department of Obstetrics and Gynecology of Kyoto University Hospital were enrolled in this study between 1993 and 2003. Expression of MICA/B, ULBP2, and CD57 in ovarian cancer tissue and normal ovary tissue was evaluated by immunohistochemical staining, and the relationship of these results to relevant clinical patient data was analyzed. Expression of MICs, ULBP2, and HLA-class I molecules in 33 ovarian cancer cell lines and two normal ovarian epithelial cell lines, as well as levels of soluble MICs and ULBP2 in the culture supernatants, were measured.
Results Expression of MICA/B and ULBP2 was detected in 97.6 and 82.9% of ovarian cancer cells, respectively, whereas neither was expressed on normal ovarian epithelium. The expression of MICA/B in ovarian cancer was highly correlated with that of ULBP2. Strong expression of ULBP2 in ovarian cancer cells was correlated with less intraepithelial infiltration of T cells and bad prognoses for patients, suggesting that ULBP2 expression is a prognostic indicator in ovarian cancer. The expression of NKG2D ligands did not correlate with the levels of the soluble forms of the ligands.
Conclusions High expression of ULBP2 is an indicator of poor prognosis in ovarian cancer and may relate to T cell dysfunction in the tumor microenvironment.

Keywords Ovarian cancer · Tumor immunology · NKG2D ligand · MICA/B · ULBP2

This work was supported by grants from Grant-in-Aid for Scientific Research (19390426, 19591932, 18209052 and 19659421) from the Ministry of Education, Science, Sports, Culture and Technology of Japan.

Electronic supplementary material The online version of this article (doi:10.1007/s00262-008-0585-3) contains supplementary material, which is available to authorized users.

K. Li · M. Mandai (✉) · J. Hamanishi · N. Matsumura · A. Suzuki · H. Yagi · K. Yamaguchi · T. Baba · I. Konishi
Department of Gynecology and Obstetrics,
Kyoto University Graduate School of Medicine,
54 Shogoin Kawahara-cho, Sakyo-ku, Kyoto 606-8507, Japan
e-mail: mandai@kuhp.kyoto-u.ac.jp

K. Li
Department of Gynecology and Obstetrics,
Peking University First Hospital, 1 Xi'an Men Street,
Xicheng District, 100034 Beijing, China

S. Fujii
Department of Obstetrics and Gynecology,
National Hospital Organization, Kyoto Medical Center,
1-1, Fukakusa Mukaihata-cho, Fushimi-ku,
Kyoto 612-8555, Japan

Introduction

Ovarian cancer is the leading cause of death among malignant gynecological tumors. Although a combination of surgery and chemotherapy has significantly improved patient survival, a majority of patients with advanced disease eventually die due to recurrence and progression. It is thus necessary to develop novel therapeutic approaches to treat ovarian cancer.

In the last decade, much research has focused on immunological aspects of malignant tumors. We have reported that $CD8^+$ T lymphocyte infiltration in ovarian cancer is associated with good prognoses [13]. Natural killer (NK) cell infiltration has also been reported to correlate with

good prognoses in some other carcinomas [17, 19, 35]. Natural killer group 2, member D (NKG2D) is a well-studied immune receptor expressed on NK cells, $CD8^+$ cytotoxic T cells and $\gamma\delta$-T cells [1, 10, 11, 33]. It is a type II transmembrane-anchored glycoprotein that is expressed as a disulfide-linked homodimer on the cell surface. NKG2D acts as an activating receptor after ligand binding, supporting the cytotoxic activity of NK cells and T cells against tumor cells [1, 4, 10, 20, 22, 25, 26].

Major histocompatibility complex class I-related chains (MIC) A and B and UL-16 binding proteins (ULBPs) are the ligands of NKG2D. They are rarely expressed by normal cells. It has been reported that MICA and MICB are constitutively expressed by intestinal epithelial cells [9, 10], and are broadly expressed in a variety of malignancies [11, 26, 31]. In malignant gliomas, MICA and ULBP2 expressions decreased with increasing WHO grade [7]. MICA expression is reported to be an indicator of good prognoses in colorectal cancer [37]. Tumor cells stably transfected to express MICA and the murine versions of the NKG2D ligands, RAE-1 or H60, at high levels, are rejected by $CD8^+$ T cells and/or NK cells [2, 5, 8, 14], which indicates that tumor cells overexpressing NKG2D ligands become more sensitive to immune cell-mediated cytolysis.

MICA/B and ULBP2 can be cleaved by matrix metalloproteases and released into the bloodstream or tissue culture medium as soluble molecules [12, 30, 31, 36]. These soluble molecules have been correlated with metastasis, advanced clinical stages of disease, and bad prognoses [15, 16, 28, 34], possibly due to their directly blocking NKG2D function or down-regulating NKG2D expression in lymphocytes. Expression of soluble MICA/B and ULBP2 by tumor cells may represent an immune evasion mechanism that leads to the impairment of immunosurveillance by T and/or NK cells [6, 12, 30, 32].

Despite these findings, there have been a few studies on NKG2D and its ligands in ovarian cancer. In the present study, we investigated MICA/B and ULBP2 expressions in ovarian cancers to evaluate their prognostic significance and association with other clinicopathological factors. We evaluated the cell surface expression and the secretion of soluble forms of these ligands in 33 ovarian cancer cell lines and 8 patients in an attempt to investigate the mechanism how NKG2D ligands play a role in ovarian cancer biology.

Materials and methods

Patients and samples

Clinical specimens were obtained from 82 women who underwent primary operations for ovarian cancer at the Department of Obstetrics and Gynecology of Kyoto University Hospital between 1993 and 2003. General patient information is shown in Table 1. The mean age of the ovarian cancer patients was 55.3 ± 11.4 years (26–80 years), and at the end of the study, 32 (39.0%) patients had died of disease and 50 (61.0%) were alive. The mean follow-up period was 68.4 ± 39.8 months (1–154 months). Normal ovarian tissues from six patients who underwent operations for uterine leiomyoma or ovarian cysts were collected as controls. We also studied ten borderline (nine mucinous borderline adenomas and one serous/mucinous borderline adenoma) and six benign ovarian tumors (five mucinous adenomas and one serous adenoma). Also the specimens and corresponding sera of eight ovarian cancer patients were also collected (general information was shown in supplementary Table 1). Clinical data were collected by retrospective review of patient files. Patients provided written informed consent under the approval of the Ethical Committee of Kyoto University Hospital.

Immunohistochemistry

Staining was performed by the streptavidin–biotin–peroxidase method. Formalin-fixed, paraffin-embedded specimens were cut into 4 μm sections. Tissue sections were deparaffinized in xylene (3 × 5 min) and hydrated through graded ethanol (99, 95 and 85%) to water. For MICA/B and ULBP2 antigen retrieval, samples were heated in Tris–EDTA buffer (pH 8.0) at 95°C for 20 min; CD57 staining did not require antigen retrieval. To block endogenous peroxidase activity, sections were treated with 100% methanol containing 0.3% H_2O_2 for 10 min. Nonspecific IgG binding was blocked using normal rabbit serum (Nichirei, Tokyo, Japan). Sections were incubated with mouse anti-MICA/B monoclonal antibodies (Abs) (6D4, Biolegend, San Diego, CA, USA), goat anti-ULBP2 Abs (R & D Systems, Inc. Minneapolis, MN, USA), and mouse anti-CD57 monoclonal Abs (Becton Dickinson, Franklin Lakes, NJ, USA) overnight at 4°C. They were then incubated with biotinylated rabbit-anti-mouse secondary Abs (Nechirei) for MICA/B and CD57 and biotinylated rabbit-anti-goat secondary Abs (Nechirei) for ULBP2, followed by incubation with a streptavidin–perioxidase solution for 30 min. Signals were generated by incubation with 3, 3′-diaminobenzidine. Finally, sections were counterstained with hematoxylin and observed under the microscope. CD8 (C8/144B, Nichirei) staining was performed as described previously [13].

Evaluation of specimens

Two independent gynecological pathologists examined the immunohistochemistry slides without any prior information about the clinical history of the patients.

Table 1 Expression of MICA/B and ULBP2, and tumor infiltration of NK and T cells according to clinico-pathological parameters (χ^2 test)

	Total	MICA/B			ULBP2			NKca			NKstroma			Tca			Tstroma		
		Low	High	*P*	Low	High	*P*	+	−	*P*	+	−	*P*	+	−	*P*	+	−	*P*
Histology	82																		
Serous	36	17	19	0.172	28	8	0.725	23	13	0.472	14	22	0.462	19	17	0.648	20	16	0.229
Clear	25	12	13		18	7		12	13		10	15		10	15		12	13	
Transition	5	4	1		3	2		3	2		3	2		4	1		4	1	
Endometrioid	11	4	7		9	2		8	3		3	8		5	6		3	8	
Undifferentiated	3	3	0		3	0		3	0		1	2		2	1		2	1	
Mucinous	2	0	2		1	1		1	1		2	0		1	1		0	2	
Age	82																		
<55	41	19	22	0.825	31	10	1.000	27	14	0.497	17	24	1.000	22	19	0.659	23	18	0.377
≥55	41	21	20		31	10		23	18		16	25		19	22		18	23	
LN metastasis	81																		
Negative	61	31	30	0.448	46	15	1.000	36	25	0.793	24	37	1.000	30	31	1.000	28	33	0.312
Positive	20	8	12		15	5		13	7		8	12		10	10		12	8	
Stage	82																		
I	29	16	13	0.493	20	9	0.628	15	14	0.551	12	17	0.543	18	11	0.079	13	16	0.300
II	5	1	4		4	1		3	2		1	4		0	5		1	4	
III	33	15	18		25	8		21	12		12	21		16	17		20	13	
IV	15	8	7		13	2		11	4		8	7		7	8		7	8	

NKca, Intra-epithelial infiltration by NK cells; NKstroma, intra-stromal infiltration by NK cells; Tca, intra-epithelial infiltration by T cells; Tstroma, intra-stromal infiltration by T cells

MICA/B and ULBP2 expressions were evaluated according to staining intensity and scored as follows: 0, negative, no staining in cancer cells (same or weaker than the cancer stroma); 1, weak expression, the staining of the cancer cells is a little stronger than that of the cancer stroma in all the area, or much stronger in a limited (less than 20%) area; 2, strong expression, the staining of the cancer cells is much stronger than that of the cancer stroma in whole section. Cases with scores of 0 and 1 were defined as the low-expression group, and cases with scores of 2 were defined as the high-expression group.

CD57 staining was evaluated as follows: tumor-infiltrating $CD57^+$ NK cells were counted in microscopic fields at 200× magnification (0.0625 mm^2) and separated by their localization as intraepithelial (infiltrating into cancer nests) or intra-stromal (infiltrating within the cancer stroma). The ten fields with the most abundant infiltration were selected, and the average count was calculated. The degree of NK cell infiltration was classified into four groups: negative intraepithelial NK infiltration (<10 NK cells found in ten intraepithelial fields); positive intraepithelial NK infiltration (≥10 NK cells found in ten intraepithelial fields); negative intrastromal NK infiltration (<20 NK cells found in ten intrastromal fields); positive intrastromal NK infiltration (≥20 NK cells found in ten intrastromal fields).

CD8 staining was evaluated as previously described; <5 $CD8^+$ cells/field was scored as negative and ≥5 cells/field was scored as positive [13].

Cell culture

In total, 33 ovarian cancer cell lines and 2 normal ovarian surface epithelial cell lines (Supplementary Table 2) were cultured under the conditions recommended for each line. Each line was grown in 10 cm tissue culture dishes with 10 ml medium at 37°C and 5% CO_2. After 24 h of growth, supernatants were collected and frozen at −80°C for ELISA analysis and cells were harvested for flow cytometry.

Flow cytometry

Single-cell suspensions from tumor cell lines were analyzed for ULBP2, MICA/B and HLA-ABC expressions by staining with PE-conjugated mouse monoclonal anti-human ULBP2 (R&D), PE-conjugated mouse anti-human MICA/B (Becton Dickinson), and FITC-conjugated mouse anti-human HLA-A, B, C (Biolegend) Abs followed by analysis in a FACSCalibur flow cytometer (Becton Dickinson). The expression of the NKG2D ligands were represented by intensity of MICs and ULBP2 which were

comparative fluorescence density when compared to isotype control (log).

Elisa

Soluble MICA and MICB in culture supernatants and the sera from eight patients were detected by the human MICA, MICB DuoSet ELISA development kits (R&D) following the manufacturer's instructions. Soluble ULBP2 was detected as described previously [36]. Two non-overlapping-ULBP2-epitope anti-ULBP2 antibodies were used. Plates were coated with 2 μg/ml anti-ULBP2 monoclonal Ab (MAB1298, R&D Systems) in PBS for 1 h at 37°C, then blocked with 300 μl 10% fetal bovine serum (FBS)/PBS at 4°C overnight and washed. Afterwards, ULBP2-Fc (1298-UL, R&D Systems) and the samples were added and plates were incubated for 1 h at 37°C. After incubation, plates were washed and the detection Ab anti-ULBP2 (AF1298, R&D Systems) was added at 0.5 μg/ml in 10% FBS/PBS for 1 h at 37°C. Plates were washed and anti-goat IgG (H + L)-HRP (1:20,000 in 0.05% PBST, ZYMED Laboratories, Carlsbad, CA, USA) was added for 1 h at 37°C. Plates were washed and developed using the Tetramethylbenzidine Peroxidase Substrate System (DY994 and DY999, R&D Systems). Absorbance was measured at 450 nm.

Statistical analyses

χ^2 tests (Fisher's exact test) were used to compare rate differences. The Spearman nonparametric correlation test was used to analyze the relationships between MICA/B and ULBP2 and tumor-infiltrating $CD57^+$ NK and $CD8^+$ T cell counts. Overall and progression-free survival curves were generated by the Kaplan–Meier method and the difference between the survival curves was analyzed by a log rank test. The contribution of variables to survival was tested by multivariate analyses using the Cox proportional hazard model. Variables included MICA/B, ULBP2, tumor-infiltrating $CD57^+$ NK cell count, $CD8^+$ T cell count and other variables such as age, stage, histology, and lymph node involvement. $P < 0.05$ was considered to be statistically significant. All statistics were performed with SPSS 10.0 software (SPSS Inc. USA).

Results

MICA/B and ULBP2 are expressed in most ovarian cancers, but in fewer borderline or benign ovarian tumors

Among 82 ovarian carcinomas, 80 (97.6%) were positive for MICA/B. The number of cases for which the expression level was scored as 0, 1, and 2 was 2/82 (2.4%), 37/82 (45.1%), and 43/82 (52.4%), respectively (Fig. 1a). Among ten borderline tumors, 3/10, 3/10, and 4/10 cases scored as 0, 1, and 2, and among six benign tumors, 2/6, 3/6, and 1/6 cases scored 0, 1, and 2.

ULBP2 was expressed in 82.9% (68/82) of cases, and the expression level was scored as 0, 1, and 2 in 14/82 (17.1%), 48/82 (58.5%), and 20/82 (24.4%) cases, respectively (Fig. 1b). For the ten borderline tumors, 8/10, 2/10, and 0/10 cases were scored as 0, 1, and 2; none of the benign tumors expressed ULBP2. None of the six normal ovarian tissues expressed MICA/B or ULBP2. There was a significant correlation between MICA/B and ULBP2 expressions, $P < 0.05$ (Table 2), but there was no correlation between MICA/B or ULBP2 expressions and patient age, FIGO stage, histological subtype, or lymph node metastasis (Table 1).

ULBP2 expression correlates with poor prognoses in ovarian cancer patients

Analysis using a Kaplan–Meier curve and log rank test revealed that the overall (75 ± 12 months) and progression-free (53 ± 11 months) survival of patients with high-ULBP2 expression was significantly worse than those with low-ULBP2 expression (112 ± 8 months, 107 ± 9 months respectively), $P < 0.05$ (Fig. 2a), whereas there were no differences in overall and progression-free survival between patients with high- and low-MICA/B expression (Fig. 2b).

Tumor infiltration of $CD8^+$ T cells, but not of $CD57^+$ NK cells, has prognostic significance in ovarian cancer

Intra-epithelial infiltration of $CD57^+$ NK cells was observed in 50/82 (61.0%) ovarian carcinoma cases, and intra-stromal infiltration of NK cells was found in 33/82 (40.2%) cases (Fig. 1c). Intra-epithelial infiltration of $CD8^+$ T cells was observed in 41/82 (50.0%) cases, and intra-stromal infiltration of $CD8^+$ T cells was found in 41/82 (50.0%) cases. There was no correlation between tumor infiltration of NK cells and $CD8^+$ T cells. Furthermore, there was no correlation between tumor infiltration of NK cells or $CD8^+$ T cells and patient age, FIGO stage, histological subtype, or lymph node metastasis (Table 1).

Kaplan–Meier curve and log rank test analyses indicated that the overall survival of patients positive only for intra-stromal infiltration of NK cells (but negative for intra-epithelial infiltration) was significantly lower than those positive only for intra-epithelial infiltration of NK cells ($P < 0.05$). In contrast, there was no difference in progression-free survival between the two groups of the patients ($P > 0.05$, Fig. 2c).

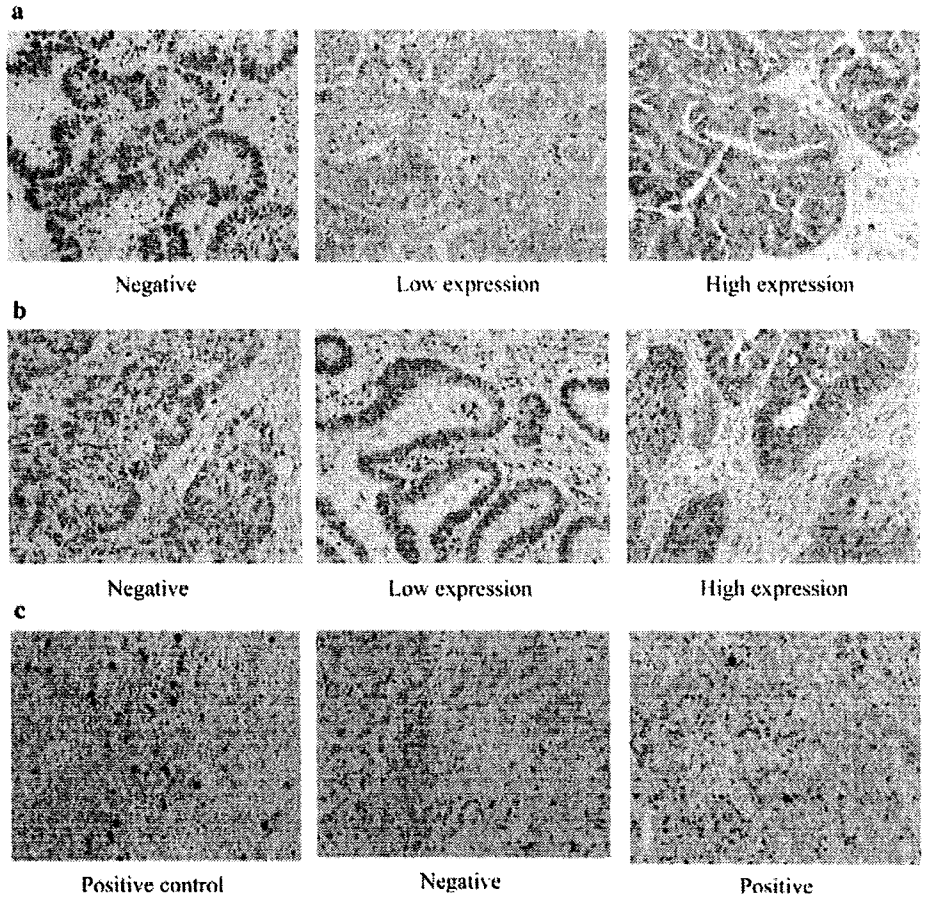

Fig. 1 Immunohistochemical staining of human ovarian cancer tissues using anti-MIC, ULBP2, and CD57 antibodies. **a** Representative staining patterns of MICs. **b** Representative staining patterns of ULBP2. **c** Representative staining patterns of $CD57^+$ NK cells. Spleens were used as positive controls (magnification, ×200)

Table 2 Correlations between NKG2D ligands and NK T cells

	MICs	NKca	NKstroma	Tca	Tstroma
n	82	82	82	82	82
MICs					
*r**	1	−0.236	−0.149	−0.190	−0.102
(*P***)		(0.033)	(0.183)	(0.088)	(0.364)
ULBP2					
*r**	0.384	−0.093	0.055	−0.220	0.014
(*P***)	(<0.001)	(0.406)	(0.626)	(0.047)	(0.898)

NKca, Intra-epithelial infiltration by NK cells; NKstroma, intra-stromal infiltration by NK cells; Tca, intra-epithelial infiltration by T cells; Tstroma, intra-stromal infiltration by T cells

* Spearman's correlation coefficient

** Significance (2-tailed)

The overall and progression-free survival of patients positive for intra-epithelial infiltration of $CD8^+$ T cells was significantly higher than those negative for intra-epithelial infiltration of T cells ($P < 0.05$), in agreement with our previous results [13].

ULBP2 expression correlates with less intra-epithelial infiltration of T cells

High expression of MICA/B in ovarian cancer cases correlated with less intra-epithelial infiltration of NK cells ($P < 0.05$), and high expression of ULBP2 correlated with less intra-epithelial infiltration of T cells ($P < 0.05$). However, there was no correlation between NKG2D ligand expression and intra-stromal infiltration of lymphocytes ($P > 0.05$, Table 2).

ULBP2 expression and intra-epithelial infiltration of T cells are independent prognostic indicators in multivariate analysis

In univariate analyses, FIGO stage, lymph node metastasis, ULBP2 expression, and intra-epithelial infiltration of T cells were prognostic indicators of both overall and progression-free survival (Table 3). High expression levels of ULBP2, FIGO stage, and lymph node metastasis correlated with poor prognoses ($P < 0.05$), whereas intra-epithelial infiltration of T cells correlated with good prognoses for patients ($P < 0.05$).

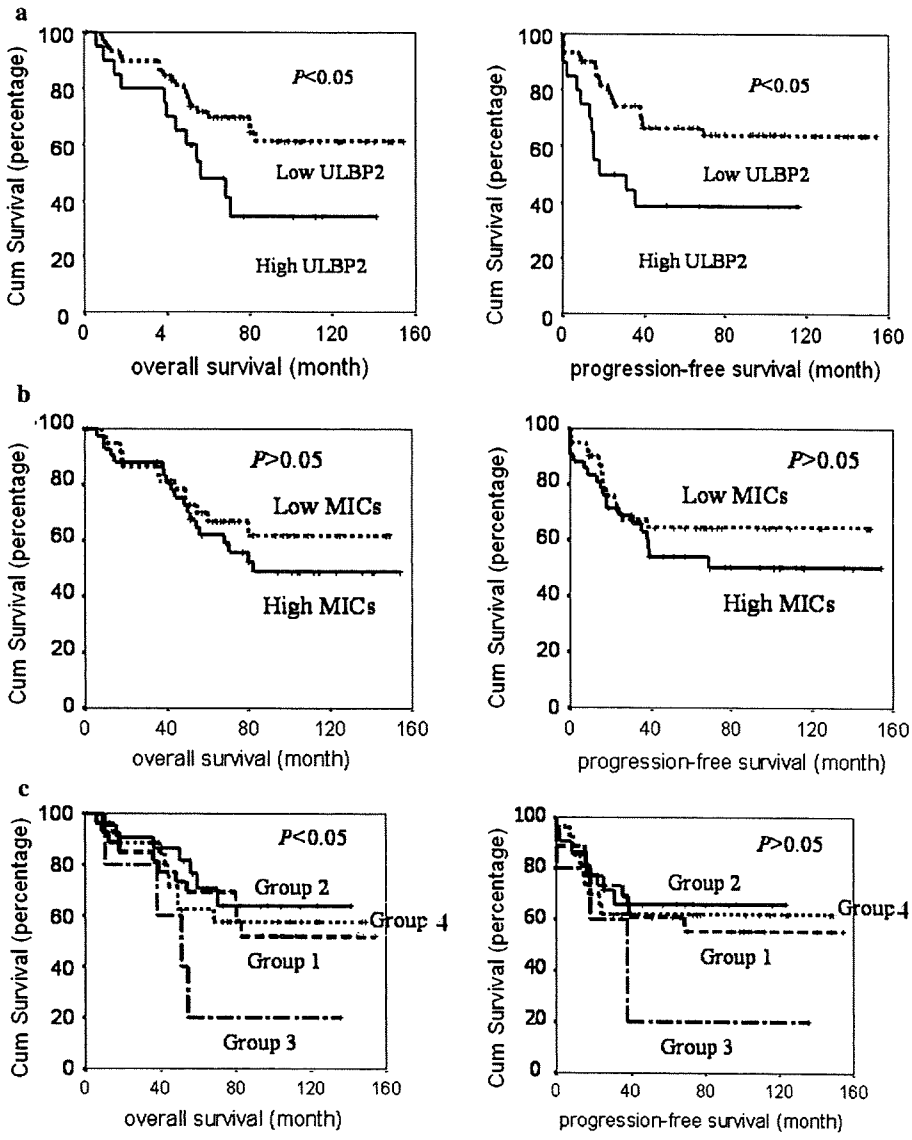

Fig. 2 Overall and progression-free survival analyses of patients with ovarian cancer according to the expression of MICA/B and ULBP2 and tumor infiltration by $CD57^+$ NK cells. **a** Kaplan–Meier curves according to high ($n = 20$) and low ($n = 62$) ULBP2 expressions. **b** Kaplan–Meier curves according to high ($n = 42$) and low ($n = 40$) MIC expressions. **c** Kaplan–Meier curves according to tumor infiltration by $CD57^+$ NK cells. Group 1 ($n = 27$), patients without tumor infiltration by NK cells; Group 2 ($n = 22$), patients only with intra-epithelial infiltration by NK cells; Group 3 ($n = 5$), patients with intra-stromal infiltration NK cells only; Group 4 ($n = 28$), patients with both intra-stromal and intra-epithelial infiltration by NK cells. The difference of overall survival between Group 2 (106 ± 11 months) and 3 (58 ± 19 months) is statistically significant, $P < 0.05$

In multivariate analyses, histology, FIGO stage, and ULBP2 expression were independent prognostic indicators of both overall and progression-free survival, whereas lymph node metastasis, intra-epithelial infiltration of T cells, and intra-stromal infiltration of NK cells were independent prognostic indicators of overall survival (Table 4). High expression of ULBP2 was an indicator of poor prognoses, whereas intra-epithelial infiltration of T cells was an indicator of good prognoses. Intra-stromal infiltration of NK cells was an indicator of poor prognoses only for overall survival.

Most ovarian cancer cell lines express cell surface and soluble forms of MICA/B and ULBP2

Among the 33 examined ovarian cancer cell lines, 32 expressed HLA-class I molecules at high levels and only ovary184 (serous adenocarcinoma) did not express it; 27/33 (81.8%) lines expressed MICA/B, and every line expressed ULBP2 (Fig. 3). None of the two normal ovarian surface epithelial cell lines expressed MICA/B, whereas both of them expressed ULBP2 at low frequencies (13.5 and 15.2% of cells, respectively). There was no correlation between the expression of MICA/B, ULBP2, or HLA ($P > 0.05$).

Soluble MICA was detected in 28/33 (84.8%) ovarian cancer cell lines (the median level is 8.5 pg/ml and the range is 0–238.9); soluble MICB was detected in 21/33 (63.6%) lines (32.5 pg/ml, 0–3095.8); soluble ULBP2 was detected in 18/33 (54.5%) lines (6.2 pg/ml, 0–97.2). No correlation was found between these results. Neither soluble MICA/B nor soluble ULBP2 was detectable in the supernatant of the two normal ovarian cell lines.

Table 3 Univariate analysis of overall and progression-free survival

Variables	Overall survival			Progression-free survival		
	P	Hazard ratio	(95% CI)	*P*	Hazard ratio	(95% CI)
Histology						
Non-clear cell	0.387	1	(0.328, 1.539)	0.360	1	(0.316, 1.519)
Clear cell		0.711			0.693	
Age						
<55	0.311	1	(0.711, 2.918)	0.408	1	(0.659, 2.793)
≥55		1.441			1.356	
Lymph node metastasis						
Negative	<0.001	1	(1.404, 2.858)	0.001	1	(1.299, 2.737)
Positive		2.003			1.886	
Stage						
I and II	<0.001	1	(2.718, 22.348)	<0.001	1	(2.631,
III and IV		7.794			7.595	21.925)
MICs						
Low	0.397	1	(0.669, 2.748)	0.311	1	(0.702, 3.032)
High		1.356			1.459	
ULBP2						
Low	0.036	1	(1.050, 4.420)	0.007	1	(1.308, 5.673)
High		2.154			2.725	
NKca						
Negative	0.383	1	(0.366, 1.470)	0.303	1	(0.335,
Positive		0.734			0.686	1.405)
NKstroma						
Negative	0.367	1	(0.685, 2.780)	0.565	1	(0.600, 2.546)
Positive		1.380			1.236	
Tca						
Negative	0.002	1	(0.139, 0.655)	0.008	1	(0.159, 0.761)
Positive		0.302			0.348	
Tstroma						
Negative	0.614	1	(0.597, 2.398)	0.696	1	(0.563, 2.364)
Positive		1.196			1.154	

NKca, Intra-epithelial infiltration by NK cells; NKstroma, intra-stromal infiltration by NK cells; Tca, intra-epithelial infiltration by T cells; Tstroma, intra-stromal infiltration by T cells

There was no correlation between the soluble levels and the cell surface expression of these NKG2D ligands (Fig. 4).

No correlation was found between the levels of soluble MICA, B and ULBP2 in the sera and their expressions in the cancer tissue of ovarian cancer patients

Soluble MICA was detected in 4/8 (50%) sera of ovarian cancer patients, the median level is 1.0 pg/ml (0, 105.5); soluble MICB was detected in 5/8 (62.5%) sera, median level is 38.3 pg/ml (0, 83.5); soluble ULBP2 was not detectable in the sera of the patients.

Among these eight ovarian carcinomas, the number of cases for which the expression level in cancer tissue was scored as 0, 1, and 2 was 1 case, 5 cases, and 2 cases, respectively. The expression level of ULBP2 was scored as 0, 1, and 2 in 1 case, 6 cases, and 1 case, respectively.

There was no correlation between the soluble levels in sera and the expressions in cancer tissue of these NKG2D ligands (Fig. 5).

Discussion

Recent studies have highlighted the significance of NKG2D function in host-mediated tumor immunity. However, the roles of the NKG2D ligands MICA/B and ULBP2 in the biology of various malignancies remain poorly understood, and the clinicopathological significance of these ligands in ovarian cancer has not yet been reported. Our study is the first to investigate the expression of MICA/B and ULBP2 in a cohort of ovarian cancer cases and a panel of ovarian cancer cell lines with well-defined histological backgrounds. We found that most ovarian cancers express

Table 4 Multivariate analysis of overall and progression-free survival

Factors	*n*	Overall survival		Progression-free survival	
		P	Hazard ratio (95%CI)	*P*	Hazard ratio (95% CI)
Histology[a]	82	0.036	3.064 (1.075, 8.733)	0.033	3.154 (1.094, 9.092)
Age[b]	82	0.819	0.913 (0.420, 1.985)	0.986	0.993 (0.448, 2.200)
Lymph node metastasis	81	0.019	1.722 (1.093, 2.714)	0.059	1.570 (0.982, 2.511)
Stage[c]	82	0.000	10.700 (3.081, 37.161)	0.000	16.029 (4.331, 59.318)
MICs	82	0.513	0.734 (0.290, 1.856)	0.181	0.490 (0.172, 1.394)
ULBP2	82	0.017	3.342 (1.240, 9.005)	0.000	7.578 (2.653, 21.647)
NKca	82	0.274	0.550 (0.188, 1.607)	0.169	0.485 (0.174, 1.358)
NKstroma	82	0.048	2.620 (1.007, 6.818)	0.063	2.525 (0.951, 6.703)
Tca	82	0.026	0.350 (0.138, 0.883)	0.117	0.476 (0.189, 1.203)
Tstroma	82	0.888	1.063 (0.458, 2.468)	0.762	1.144 (0.480, 2.727)

NKca, Intra-epithelial infiltration by NK cells; NKstroma, intra-stromal infiltration by NK cells; Tca, intra-epithelial infiltration by T cells; Tstroma, intra-stromal infiltration by T cells

[a] Patients were divided into non-clear cell carcinoma group and clear cell carcinoma group

[b] Patients were divided into younger women (<55 years) group and elder women (≥55 years) group

[c] Patients were divided into early stage (stages I and II) group and late stage (stages III and IV) group

MICA/B and ULBP2. Borderline and benign tumors expressed them to a lesser extent, but normal ovarian epithelium did not express them. These findings suggest that the expression of NKG2D ligands only occurs after malignant transformation during ovarian cancer development, which is consistent with findings for many other malignancies. Hence, these molecules have the potential to be used as tumor markers for ovarian cancer.

It is well known that the cytotoxic function of NK cells is directly activated by tumor cells, whereas $CD8^+$ T cells require simultaneous pre-sensitization and HLA stimulation. Inducible-surface expression of NKG2D ligands in response to stress or malignant transformation is thought to mark dysfunctional cells for elimination by cytotoxic lymphocytes via NKG2D-mediated mechanisms (the "induced-self" hypothesis) [1, 21, 27]. Indeed, ectopic expression of NKG2D ligands by tumors induces perforin-dependent strong NK and cytotoxic T lymphocyte (CTL) responses in vivo [5, 14]. However, in various human malignancies, including ovarian cancer, it remains unknown whether elevated NKG2D ligand expression in fact leads to enhanced tumor immunity and to better prognoses for patients. Paradoxically, in this study high ULBP2 expression correlated with poor prognoses for patients with ovarian cancer. Expression of another NKG2D ligand, MICA/B, did not correlate with prognoses, suggesting that ULBP2 rather than MICA/B might influence the clinical course of ovarian cancer.

One potential mechanism to explain why high expression of ULBP2 leads to poor prognoses may relate to the shedding of this ligand. Recent studies have shown that both MICA/B and ULBP2 on the cell membrane may be proteolytically cleaved by metalloproteases to produce soluble molecules [12, 14, 30, 36]. These soluble forms systemically down-regulate the surface expression of NKG2D receptors, thereby impairing the anti-tumor reactivity of NK and $CD8^+$ T cells [6, 12]. Taking these results into account, we measured soluble MICA/B and ULBP2 levels in the supernatants of ovarian cancer cell lines and examined whether these levels correlate with the expression levels of NKG2D ligands on the same cells. Our results show that ovarian cancer cells indeed secrete various amounts of soluble NKG2D ligands. However, no correlation was found between the secreted NKG2D ligand levels as measured by ELISA and the expression levels of these ligands on the surface of the cells as detected by flow cytometry. We also collected paired samples of sera and cancer specimen of eight ovarian cancer patients and compared the expression levels of NKG2D ligands. Again, there was no correlation between the soluble molecules levels and cancer tissue expression in vivo (even there was no detectable soluble ULBP2 in sera in accordance with previous report on gastrointestinal malignancies and healthy donors [36]). A recently published report showed that soluble MICA levels in ovarian cancer patients were significantly higher than that in normal women, but no correlation was found between elevated levels of soluble MICA and cancer stage or metastasis [15]. These findings altogether suggest that secreted soluble NKG2D ligands are not responsible for the poor prognosis of the ovarian cancer patient.

To evaluate the influence of NKG2D ligand expression on the immunological microenvironment in ovarian cancer, we investigated the infiltration of both $CD8^+$ T and $CD57^+$ NK cells in the same ovarian cancer tissues. Overexpres-

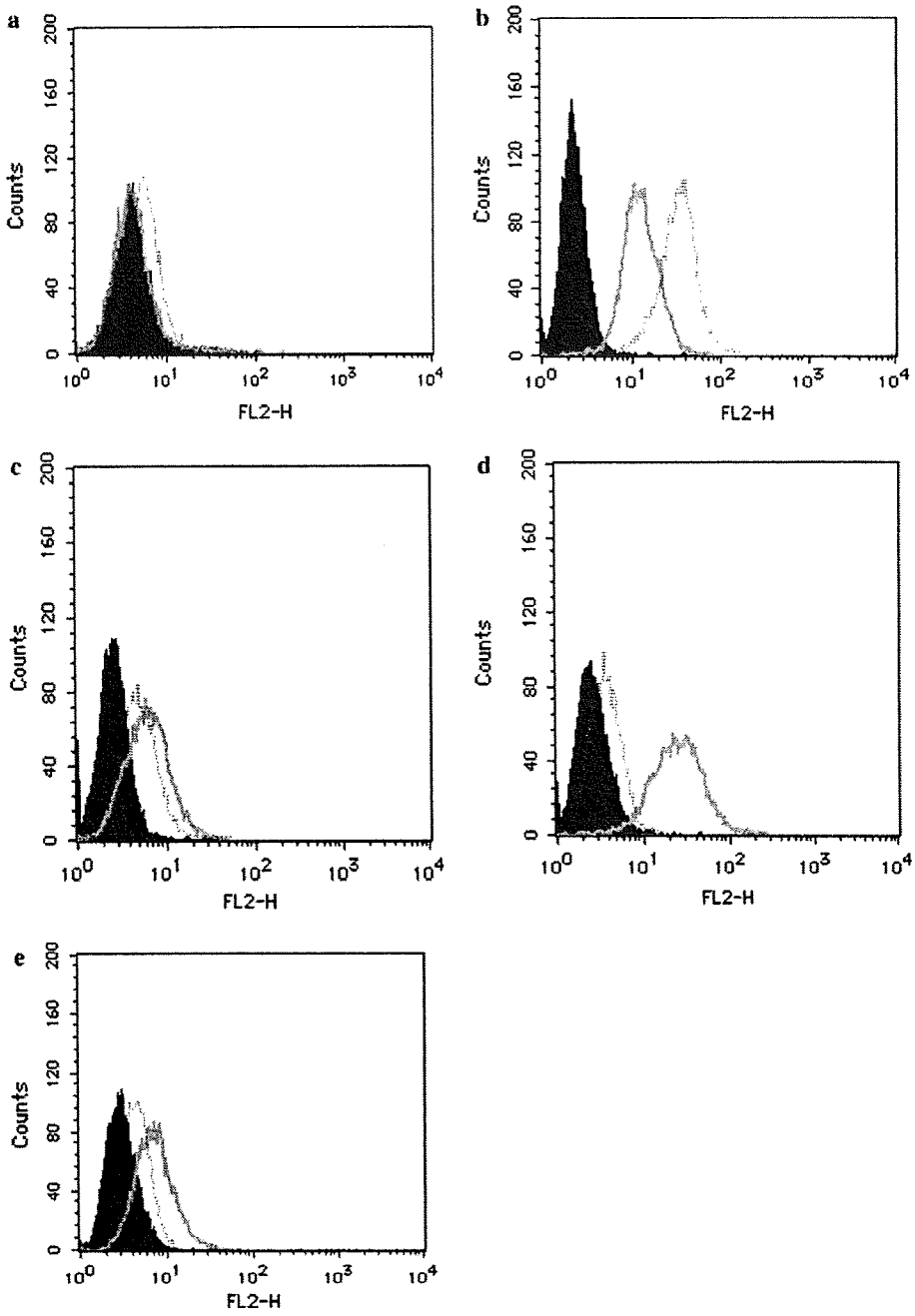

Fig. 3 Representative flow cytometry results for ovarian cell lines. The figure shows the expression of MICs (*solid line*) and ULBP2 (*dot line*), the *filled histograms* represent the isotype control. **a** Normal ovarian cell line OSE6. **b** Endometrioid adenocarcinoma cell line OV2008. **c** Serous adenocarcinoma cell line OVCAR-3. **d** Clear cell carcinoma cell line TOV-21G. **e** Undifferentiated carcinoma cell line A2780

sion of ULBP2 correlated with less tumor infiltration by $CD8^+$ T cells, but not with infiltration of $CD57^+$ NK cells. Furthermore, tumor infiltration of $CD8^+$ T cells correlated with patient prognoses, whereas tumor infiltration of $CD57^+$ NK cells did not correlate with the prognosis of ovarian cancer.

Altogether, these findings suggest that in ovarian cancer, overexpression of ULBP2 rather than MICA/B might hinder the infiltration of cytotoxic T lymphocytes and lead to an unfavorable clinical course by allowing tumor cells to escape from immune surveillance, and this effect may not be induced by the soluble types of the NKG2D ligands. Recently, two mechanisms to explain the link between NKG2D ligand expression and immune dysfunction have been proposed. Chronic engagement of NK cells with NKG2D ligands expressed by tumor cells in vitro and in vivo might not only impair NKG2D function, but also might suppress most of the cytotoxic functions of NK cells [3, 24, 38]. Other reports have shown that MICA/B on target cells can be transferred to NK cells upon conjugation

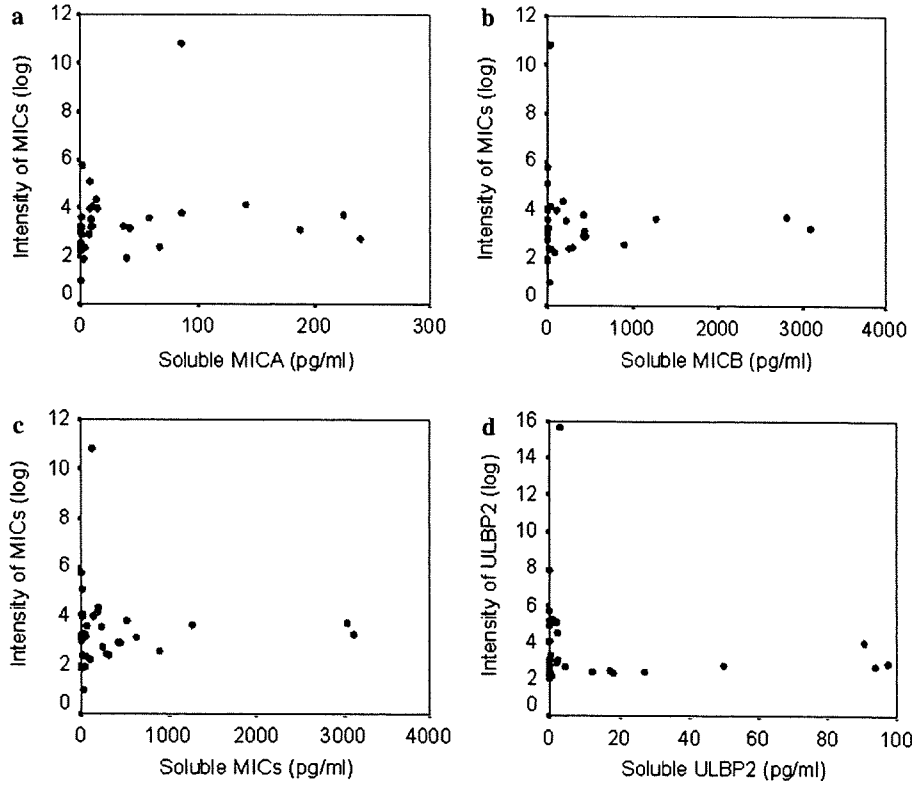

Fig. 4 The relationship between the ligands expression on the cell membrane and the soluble molecules levels in supernatant of ovarian cancer cell lines. *X*-axis represents soluble NKG2D ligands in supernatant which was detected by ELISA. *Y*-axis represents expression of NKG2D ligands detected by flow cytometry, which is shown as comparative fluorescence density compared to isotype control (log). **a** There was no correlation between the soluble MICA and the cell surface expression of MICs. **b** There was no correlation between the soluble MICB and the cell surface expression of MICs. **c** There was no correlation between the soluble MICs (sum of the soluble MICA and MICB) and the cell surface expression of MICs. **d** There was no correlation between the soluble ULBP2 and the cell surface expression of ULBP2

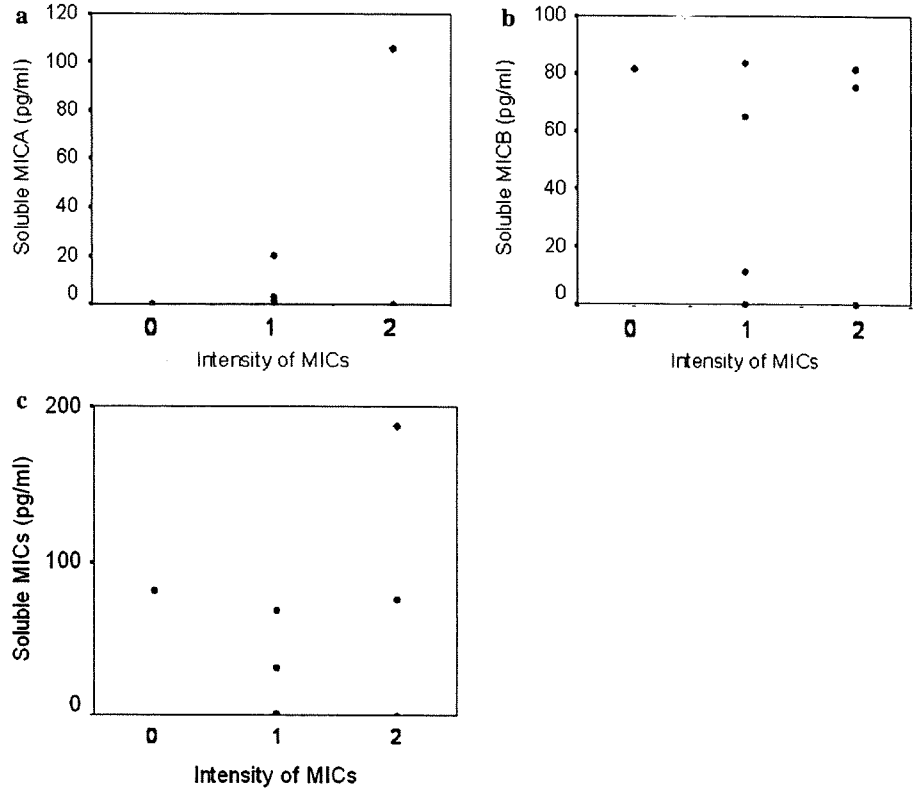

Fig. 5 The relationship between the immunohistochemical expression of MICA/B in the cancer tissue (*x*-axis) and the soluble molecules levels in sera of ovarian cancer patients (*y*-axis). **a** There was no correlation between the soluble MICA and the cancer expression of MICs. **b** There was no correlation between the soluble MICB and the cancer expression of MICs. **c** There was no correlation between the soluble MICs (sum of the soluble MICA and MICB) and the cancer expression of MICs. Intensity of MICs: *0* negative expression, *1* weak expression and *2* strong expression in immunohistochemistry

with NKG2D, and that transferred MICA/B might further down-regulate NKG2D expression in surrounding NK cells or result in cytolysis of the affected NK cells by other NK cells [23, 29]. Similar phenomena have been observed in T cells [18]. Importantly, these effects were mainly caused by cell–cell contact, and the soluble forms of the ligands had little effect [3, 24, 38]. Although direct evidence has not been provided, mechanisms similar to these might explain our finding that elevated ULBP2 expression was associated with less $CD8^+$ T cell infiltration and poor prognoses.

In summary, we show here for the first time that most ovarian cancers express NKG2D ligands, and that strong expression of ULBP2 correlates with poor prognoses for patients, possibly due to the functional inhibition of $CD8^+$ T cells. We have previously reported that intratumoral $CD8^+$ T cells are indicators of poor prognoses in ovarian cancer patients, and the findings described here might partly explain those results. Further investigation is necessary to determine whether the connection between ULBP2 and NKG2D regulates tumor immunity in ovarian cancer and whether it is the exact mechanism underlying this connection.

Acknowledgments The authors thank Dr. Aoki, Keio University Japan; Dr. Saga, Jichi Medical University Japan; Dr. Hirahara, Yokohama City University Japan; Dr. Berchuck and Dr. Murphy, Duke University USA for kindly providing ovarian cell lines.

References

1. Bauer S, Groh V, Wu J, Steinle A, Phillips JH, Lanier LL, Spies T (1999) Activation of NK cells and T cells by NKG2D, a receptor for stress-inducible MICA. Science 285:727–729
2. Busche A, Goldmann T, Naumann U, Steinle A, Brandau S (2006) Natural killer cell-mediated rejection of experimental human lung cancer by genetic overexpression of major histocompatibility complex class I chain-related gene A. Hum Gene Ther 17:135–146
3. Coudert JD, Scarpellino L, Gros F, Vivier E, Held W (2008) Sustained NKG2D engagement induces cross-tolerance of multiple distinct NK cell activation pathways. Blood 111(7):3571–3578
4. Das H, Groh V, Kuijl C, Sugita M, Morita CT, Spies T, Bukowski JF (2001) MICA engagement by human $V\gamma2V\delta2$ T cells enhances their antigen-dependent effector function. Immunity 15:83–93
5. Diefenbach A, Jensen ER, Jamieson AM, Raulet DH (2001) Rae1 and H60 ligands of the NKG2D receptor stimulate tumour immunity. Nature 413:165–171
6. Doubrovina ES, Doubrovin MM, Vider E et al (2003) Evasion from NK cell immunity by MHC class I chain-related molecules expressing colon adenocarcinoma. J Immunol 171:6891–6899
7. Eisele G, Wischhusen J, Mittelbronn M, Meyermann R, Waldhauer I, Steinle A, Weller M, Friese MA (2006) TGF-beta and metalloproteinases differentially suppress NKG2D ligand surface expression on malignant glioma cells. Brain 129(Pt9):2416–2425
8. Friese MA, Platten M, Lutz SZ, Naumann U, Aulwurm S, Bischof F, Buhring HJ, Dichgans J, Rammensee HG, Steinle A, Weller M (2003) MICA/NKG2D mediated immunogene therapy of experimental gliomas. Cancer Res 63:8996–9006
9. Groh V, Bahram S, Bauer S, Herman A, Beauchamp M, Spies T (1996) Cell stress-regulated human major histocompatibility complex class I gene expressed in gastrointestinal epithelium. Proc Natl Acad Sci USA 93:12445–12450
10. Groh V, Steinle A, Bauer S, Spies T (1998) Recognition of stress-induced MHC molecules by intestinal epithelial $\gamma\delta$T cells. Science 279:1737–1740
11. Groh V, Rhinehart R, Secrist H, Bauer S, Grabstein KH, Spies T (1999) Broad tumor-associated expression and recognition by tumor-derived $\gamma\delta$T cells of MICA and MICB. Proc Natl Acad Sci USA 96:6879–6884
12. Groh V, Wu J, Yee C, Spies T (2002) Tumour-derived soluble MIC ligands impair expression of NKG2D and T-cell activation. Nature 419:734–738
13. Hamanishi J, Mandai M, Iwasaki M, Okazaki T, Tanaka Y, Yamaguchi K, Higuchi T, Yagi H, Takakura K, Minato N, Honjo T, Fujii S (2007) Programmed cell death 1 ligand 1 and tumor-infiltrating CD8+ T lymphocytes are prognostic factors of human ovarian cancer. Proc Natl Acad Sci USA 104:3360–3365
14. Hayakawa Y, Kelly JM, Westwood JA, Darcy PK, Diefenbach A, Raulet D, Smyth MJ (2002) Cutting edge: tumor rejection mediated by NKG2D receptor ligand interaction is dependent upon perforin. J Immunol 169:5377–5381
15. Holdenrieder S, Stieber P, Peterfi A, Nagel D, Steinle A, Salih RH (2006) Soluble MICA in malignant diseases. Int J Cancer 118:684–687
16. Holdenrieder S, Stieber P, Peterfi A, Nagel D, Steinle A, Salih RH (2006) Soluble MICB in malignant diseases: analysis of diagnostic significance and correlation with soluble MICA. Cancer Immunol Immunother 55:1284–1289
17. Hsia JY, Chen JT, Chen CY, Hsu CP, Miaw J, Huang YS, Yang CY (2005) Prognostic significance of intratumoral natural killer cells in primary resected esophageal squamous cell carcinoma. Chang Gung Med J 28:335–340
18. Huang JF, Yang Y, Sepulveda H, Shi W, Hwang I, Peterson PA, Jackson MR, Sprent J, Cai Z (1999) TCR-Mediated internalization of peptide–MHC complexes acquired by T cells. Science 286:952–954
19. Ishigami S, Natsugoe S, Tokuda K, Nakajo A, Che X, Iwashige H, Aridome K, Hokita S, Aikou T (2000) Prognostic value of intratumoral natural killer cells in gastric carcinoma. Cancer 88:577–583
20. Jamieson AM, Diefenbach A, McMahon CW, Xiong N, Carlyle JR, Raulet DH (2002) The role of the NKG2D immunoreceptor in immune cell activation and natural killing. Immunity 17:19–29
21. Lanier LL (2001) A renaissance for the tumor immunosurveillance hypothesis. Nat Med 7:1178–1180
22. Maccalli C, Pende D, Castelli C, Mingari MC, Robbins PF, Parmiani G (2003) NKG2D engagement of colorectal cancer-specific T cells strengthens TCR mediated antigen stimulation and elicits TCR independent anti-tumor activity. Eur J Immunol 33:2033–2043
23. McCann FE, Eissmann P, Onfelt B, Leung R, Davis DM (2007) The activating NKG2D ligand MHC class I-related chain A transfers from target cells to NK cells in a manner that allows functional consequences. J Immunol 178:3418–3426
24. Oppenheim DE, Roberts SJ, Clarke SL et al (2005) Sustained localized expression of ligand for the activating NKG2D receptor impairs natural cytotoxicity in vivo and reduces tumor immunosurveillance. Nat Immunol 6:928–937
25. Pende D, Cantoni C, Rivera P, Vitale M, Castriconi R, Marcenaro S, Nanni M, Biassoni R, Bottino C, Moretta A, Moretta L (2001) Role of NKG2D in tumor cell lysis mediated by human NK cells: cooperation with natural cytotoxicity receptors and capability of recognizing tumors of nonepithelial origin. Eur J Immunol 31:1076–1086
26. Pende D, Rivera P, Marcenaro S, Chang CC, Biassoni R, Conte R, Kubin M, Cosman D, Ferrone S, Moretta L, Moretta A (2002) Major histocompatibility complex class I-related chainA and

UL16-binding protein expression on tumor cell lines of different histotypes: analysis of tumor susceptibility to NKG2D dependent natural killer cell cytotoxicity. Cancer Res 62:6178–6186
27. Raulet DH (2003) Roles of the NKG2D immunoreceptor and its ligands. Nat Rev Immunol 3:781–790
28. Rebmann V, Schutt P, Brandhorst D, Opalka B, Moritz T, Nowrousian MR, Grosse-Wilde H (2007) Soluble MICAs an independent prognostic factor for the overall survival and progression-free survival of multiple myeloma patients. Clin Immunol 123:114–120
29. Roda-Navarro P, Vales-Gomez M, Chisholm SE, Reyburn HT (2006) Transfer of NKG2D and MICB at the cytotoxic NK cell immune synapse correlates with a reduction in NK cell cytotoxic function. Proc Natl Acad Sci USA 103:11258–11263
30. Salih HR, Rammensee HG, Steinle A (2002) Cutting edge: down-regulation of MICA on human tumors by proteolytic shedding. J Immunol 169:4098–4102
31. Salih HR, Antropius H, Gieseke F, Lutz SZ, Kanz L, Rammensee HG, Steinle A (2003) Functional expression and release of ligands for the activating immunoreceptor NKG2D in leukemia. Blood 102:1389–1396
32. Song H, Kim JK, Cosman D, Choi I (2006) Soluble ULBP suppresses natural killer cell activity via down-regulating NKG2D expression. Cell Immunol 239:22–30
33. Steinle A, Groh V, Spies T (1998) Diversification, expression, and $\gamma\delta$T cell recognition of evolutionarily distant members of the MIC family of major histocompatibility complex class I-related molecules. Proc Natl Acad Sci USA 95:12510–12515
34. Vetter CS, Lieb W, Brocker E-B, Becker JC (2004) Loss of nonclassical MHC molecules MIC-A/B expression during progression of uveal melanoma. Br J Cancer 91:1495–1499
35. Villegas FR, Coca S, Villarrubia VG, Jiménez R, Chillón MJ, Jareño J, Zuil M, Callol L (2002) Prognostic significance of tumor infiltrating natural killer cells subset CD57 in patients with squamous cell lung cancer. Lung Cancer 35:23–28
36. Waldhauer I, Steinle A (2006) Proteolytic release of soluble UL16-binding protein 2 from tumor cells. Cancer Res 66:2520–2526
37. Watson NF, Spendlove I, Madjd Z, McGilvray R, Green AR, Ellis IO, Scholefield JH, Durrant LG (2006) Expression of the stress-related MHC class I chain-related protein MICA is an indicator of good prognosis in colorectal cancer patients. Int J Cancer 118:1445–1452
38. Wiemann K, Mittrücker HW, Feger U, Welte SA, Yokoyama WM, Spies T, Rammensee HG, Steinle A (2005) Systemic NKG2D down-regulation impairs NK and CD8 T cell responses in vivo. J Immunol 175:720–729

Jpn J Clin Oncol 2010;40(1)36–41
doi:10.1093/jjco/hyp127
Advance Access Publication 10 October 2009

The Optimal Debulking after Neoadjuvant Chemotherapy in Ovarian Cancer: Proposal Based on Interval Look During Upfront Surgery Setting Treatment

Takashi Onda[1,2], Hiroyuki Yoshikawa[1,3], Toshiharu Yasugi[1,4], Koji Matsumoto[1,3] and Yuji Taketani[1]

[1]Department of Obstetrics and Gynecology, Faculty of Medicine, University of Tokyo, [2]Division of Gynecologic Oncology, National Cancer Center Hospital, Tokyo, [3]Department of Obstetrics and Gynecology, University of Tsukuba, Ibaraki and [4]Department of Gynecology, Tokyo Metropolitan Cancer and Infectious diseases Center Komagome Hospital, Tokyo, Japan

For reprints and all correspondence: Takashi Onda, Division of Gynecologic Oncology, National Cancer Center Hospital, 5-1-1 Tsukiji, Chuo-ku, Tokyo 104-0045, Japan. E-mail: taonda@ncc.go.jp

Received May 29, 2009; accepted August 29, 2009

Objective: The optimal goal of interval debulking surgery (IDS) following neoadjuvant chemotherapy (NAC) remains undefined. The aim of this study was to determine the optimal goal of IDS following NAC on the basis of long-term survival by the disease status at the end of interval look surgery (ILS) or IDS during the treatment in the setting of upfront primary debulking surgery (PDS).

Methods: From January 1986 through December 2000, we performed treatment in the setting of upfront PDS in 128 patients with Stage III/IV epithelial ovarian cancer. Sixty-six patients with residual disease (RD) at PDS underwent interval surgery (IS) such as ILS or IDS; 4 patients after two cycles of chemotherapy and 62 after three or more cycles. We investigated how disease status at the end of IS was associated with overall survival (OS).

Results: The 5-year OS rates for no, minimal and gross RD were not available ($n = 0$), 67% ($n = 3$) and 0% ($n = 1$) after two cycles, and 47% ($n = 42$), 0% ($n = 18$) and 0% ($n = 2$) after three or more cycles, respectively. No visible tumors at the end of IS after three or more cycles of chemotherapy were necessary for 5-year survival.

Conclusions: If the optimal goal of IDS is defined as the surgery that is expected to result in long-term survival in the NAC setting treatment, our data on the assessment of peritoneal findings during the upfront PDS setting treatment suggest that only complete resection with no RD could be the optimal goal of IDS in the NAC setting treatment.

Key words: ovarian cancer – neoadjuvant therapy – gynecol-surg – chemo-gynecology

INTRODUCTION

Primary debulking surgery (PDS) followed by chemotherapy is a standard treatment for ovarian cancer. For patients with advanced ovarian cancer, the goal of PDS is optimal cytoreduction, usually defined as surgery with residual disease (RD) <1 or <2 cm in diameter. Proportion of patients who achieved optimal surgery or size of RD is one of the important prognostic factors for the patients with advanced ovarian cancer (1–4). Unfortunately, optimal cytoreduction for advanced ovarian cancer is achieved in only 30–60% of the patients at most institutions (5,6). One reason for this low rate is that patients with advanced ovarian cancer are often poor candidates for aggressive surgery because of low performance status (PS) caused by massive ascites, pleural effusion and large abdominal tumors. Another reason is that some patients have unresectable tumors at the time of primary surgery.

Thus, because of recent advances in chemotherapy, neoadjuvant chemotherapy (NAC) followed by interval debulking surgery (IDS) and further chemotherapy has become an alternative treatment for patients with low PS and those with apparently unresectable tumors evaluated with computed

tomography (CT) or laparoscopy. Several retrospective studies revealed comparable results by the NAC setting treatments with standard treatment (7–9), and a few prospective Phase II (10) or feasibility study (11,12) revealed promising results by NAC setting treatment. Taking into account these favorable outcomes of NAC setting treatment, several prospective clinical trials are now under way to compare this treatment with the standard treatment for advanced ovarian cancer, not only in patients with low PS or unresectable tumors (13,14). Most previous studies have emphasized that the greatest advantage of the treatment in the setting of an NAC is a higher rate of optimal cytoreduction at IDS (7,9,10). These studies used the same definition of optimal cytoreduction at IDS as that at PDS. At the time of PDS, optimal cytoreduction indicates an optimal goal of surgery that lengthens survival. However, there is limited information on the survival of patients in relation to the size of RD after IDS. Thus, the appropriate definition of 'optimal cytoreduction' at the time of IDS in the setting of NAC is undetermined.

Since 1986, we have performed interval look surgery (ILS) for patients who have minimal RD (<2 cm in diameter) at PDS or IDS for patients who have gross RD (≥2 cm in diameter) at PDS after two to six cycles (mostly three or four cycles) of chemotherapy. We investigated how peritoneal findings at the end of interval surgery (IS) are associated with the overall survival (OS) of patients. These associations should help us to clarify the optimal goal of IDS in the setting of NAC for advanced ovarian cancer.

PATIENTS AND METHODS

Patients

From January 1986 through December 2000, we treated 230 patients with epithelial ovarian cancer, including 128 patients with Stage III–IV disease, at the Department of Obstetrics and Gynecology, University of Tokyo Hospital. According to the International Federation of Gynecology and Obstetrics (FIGO) staging, disease was classified as Stage IIIB in 14 patients, Stage IIIC in 89 patients and Stage IV in 25 patients. Histologic type was serous in 94 patients, clear cell in 18 patients, endometrioid in 6 patients, mucinous in 5 patients, transitional cell in 2 patients, mixed epithelial in 2 patients and undifferentiated in 1 patient. Median age at the time of PDS was 54 years, with a range of 29–78 years. Median follow-up period after PDS, excluding patients who died, was 94 months, with a range of 8–201 months. All but two surviving patients were followed up for >5 years.

Our standard surgical treatment for advanced ovarian cancer at the time of PDS consists of total abdominal hysterectomy, bilateral salpingo-oophorectomy, infracolic or total omentectomy, and debulking of peritoneal tumor masses with maximum efforts. Patients with no or minimal RD (<2 cm in diameter) also underwent systematic retroperitoneal lymphadenectomy, except for patients with severe medical complications, low PS or long operation time. Retroperitoneal lymphadenectomy included both the pelvic and aortic lymph nodes.

In principle, our primary management for ovarian cancer was performed as follows according to the outcome of PDS: (i) patients with no RD received six cycles of chemotherapy and underwent no additional surgery, (ii) patients with minimal RD (<2 cm in diameter) received three or four cycles of chemotherapy followed by ILS and two to four cycles of additional chemotherapy, (iii) patients with gross RD (≥2 cm in diameter) received two to four cycles of chemotherapy until a favorable response was obtained and underwent IDS followed by four to five cycles of additional chemotherapy.

Cisplatin-based regimens, such as CAP or TC, were used for post-operative chemotherapy. From 1986 through 1997, we used the CAP regimen, consisting of 400–600 mg/m^2 of cyclophosphamide, 30–40 mg/m^2 of doxorubicin and 50–75 mg/m^2 of cisplatin. Thereafter, we used the TC regimen consisting of paclitaxel (175 mg/m^2 infused over 3 h) and an area under the curve 6 of carboplatin.

Statistical Methods

OS was measured from the day of starting primary treatment. The survival curves were determined with the Kaplan–Meier product-limit method. Differences in survival were analyzed with the log-rank test and Cox proportional-hazard regression model using the SPSS program ver. 11.0 (SPSS Inc., Chicago, IL, USA).

RESULTS

Survival of all Patients in Relation to the Size of RD at PDS

In 128 patients with Stage III or IV ovarian cancer, complete resection of all visible tumors was achieved in 37 patients (28.9%), minimal RD remained in 52 patients (40.6%) and gross RD remained in 39 patients (30.5%). Figure 1 shows the OS of all 128 patients with Stage III/IV disease in relation to the largest size of RD at PDS. Median OSs and 5-year OS rates of the above three groups were 112 months and 65%, 50 months and 40%, and 22 months and 13%. The difference in OS among the three groups was statistically significant ($P < 0.0001$ with log-rank test). In particular, the difference in OS between patients with minimal RD and gross RD was more significant than that between patients with no RD and minimal RD ($P < 0001$ vs. $P = 0.02$). Hazard ratio and 95% confidence interval (CI) for patients with minimal RD and gross RD against patients with no RD were 1.92 (1.08–3.42) and 5.43 (2.98–9.89), respectively.